

Analytical Modeling and Thermodynamic Analysis of Robust Superhydrophobic Surfaces with Inverse-Trapezoidal Microstructures

Maesoon Im,[†] Hwon Im, Joo-Hyung Lee, Jun-Bo Yoon, and Yang-Kyu Choi*

Department of Electrical Engineering, KAIST, 335 Gwahangno, Yuseong-gu, Daejeon 305-701, Republic of Korea. [†]Present address: Department of Electrical Engineering and Computer Science, University of Michigan, Ann Arbor, MI 48109-2122, United States.

Received March 16, 2010. Revised Manuscript Received September 9, 2010

A polydimethylsiloxane (PDMS) elastomer surface with perfectly ordered microstructures having an inverse-trapezoidal cross-sectional profile (simply PDMS trapezoids) showed superhydrophobic and transparent characteristics under visible light as reported in our previous work. The addition of a fluoropolymer (Teflon) coating enhances both features and provides oleophobicity. This paper focuses on the analytical modeling of the fabricated PDMS trapezoids structure and thermodynamic analysis based on the Gibbs free energy analysis. Additionally, the wetting characteristics of the fabricated PDMS trapezoids surface before and after the application of the Teflon coating are analytically explained. The Gibbs free energy analysis reveals that, due to the Teflon coating, the Cassie–Baxter state becomes energetically more favorable than the Wenzel state and the contact angle difference between the Cassie–Baxter state and the Wenzel state decreases. These two findings support the robustness of the superhydrophobicity of the fabricated Teflon-coated PDMS trapezoids. This is then verified via the impinging test of a water droplet at a high speed. The dependencies of the design parameters in the PDMS trapezoids on the hydrophobicity are also comprehensively studied through a thermodynamic analysis. Geometrical dependency on the hydrophobicity shows that overhang microstructures do not have a significant influence on the hydrophobicity. In contrast, the intrinsic contact angle of the structural material is most important in determining the apparent contact angle. On the other hand, the experimental results showed that the side angles of the overhangs are critical not for the hydrophobic but for the oleophobic property with liquids of a low surface tension. Understanding of design parameters in the PDMS trapezoids surface gives more information for implementation of superhydrophobic surfaces.

1. Introduction

Superhydrophobic surfaces have been studied extensively for a wide variety of applications, such as self-cleaning surfaces¹ and microfluidic systems.² It is well-known that the hydrophobicity of a surface is a function of its chemical characteristics^{3,4} and of its physical characteristics.^{5,6} Given the limitations in enhancing the hydrophobic property of a flat surface with the aid of chemical modification,⁴ physical modifications to instill various rough surfaces^{7–10} have been attempted. The superhydrophobic features attained by rough surfaces have been understood in terms of the Wenzel model⁵ and the Cassie–Baxter model.⁶

When a liquid droplet is placed on a rough solid surface, the wetting behavior follows either the Wenzel model⁵ or the Cassie–Baxter model,⁶ in which the thermodynamic energy of an entire system of liquid, solid, and air is minimized. The Wenzel state prevails when the surface is completely wetted (i.e., homogeneous wetting), as shown in Figure 1a. The contact angle of the liquid

droplet in the Wenzel state can be expressed by the following equation:⁵

$$\cos \theta_W = r \cos \theta_{\text{FLAT}} \quad (1)$$

In this equation, θ_W is the apparent contact angle in the Wenzel state, θ_{FLAT} is the intrinsic contact angle on a flat surface of the same material, and r is the surface roughness factor. This final variable is defined as the ratio of the actual surface area to the projected surface area. In contrast, the Cassie–Baxter state prevails when the surface is partially supported by trapped air (i.e., heterogeneous wetting) among adjacent asperities as well as by the solid surface itself, as illustrated in Figure 1b. Hence, a liquid droplet can form a composite interface. The wetting behavior in the domain of the Cassie–Baxter state⁶ is governed by the following equation:⁸

$$\cos \theta_{\text{CB}} = r_f f (\cos \theta_{\text{FLAT}}) + f - 1 \quad (2)$$

Here, θ_{CB} is the apparent contact angle in the Cassie–Baxter state, r_f is the surface roughness factor, which is defined as the ratio of the actual liquid contact area to the projected surface area, and f is the fraction of the projected surface area that makes contact with the liquid.

Among the diverse microstructures with the potential to realize a rough surface, overhang structures^{11,12} and re-entrant textures^{13,14} have been utilized in several studies to implement superhydrophobic

*To whom correspondence should be addressed. E-mail: ykchoi@ee.kaist.ac.kr. Phone: +82-42-350-3477. Fax: +82-42-350-8565.

(1) Blosssey, R. *Nat. Mater.* **2003**, *2*, 301–306.
(2) Tabeling, P. *Lab Chip* **2009**, *9*, 2428–2436.
(3) Zhuang, Y. X.; Hansen, O.; Knieling, T.; Wang, C.; Rombach, P.; Lang, W.; Benecke, W.; Kehlenbeck, M.; Koblit, J. *J. Microelectromech. Syst.* **2007**, *16*, 1451–1460.
(4) Nishino, T.; Meguro, M.; Nakamae, K.; Matsushita, M.; Ueda, Y. *Langmuir* **1999**, *15*, 4321–4323.
(5) Wenzel, R. N. *Ind. Eng. Chem.* **1936**, *28*(8), 988–994.
(6) Cassie, A. B. D.; Baxter, S. *Trans. Faraday Soc.* **1944**, *40*, 546–551.
(7) Feng, X.; Jiang, L. *Adv. Mater.* **2006**, *18*, 3063–3078.
(8) Roach, P.; Shirtcliffe, N. J.; Newton, M. I. *Soft Matter* **2008**, *4*, 224–240.
(9) Kwon, Y.; Patankar, N.; Choi, J.; Lee, J. *Langmuir* **2009**, *25*(11), 6129–6136.
(10) Jeong, H. E.; Lee, S. H.; Kim, J. K.; Suh, K. Y. *Langmuir* **2006**, *22*, 1640–1645.

(11) Ahuja, A.; Taylor, J. A.; Lifton, V.; Sidorenko, A. A.; Salamon, T. R.; Lobaton, E. J.; Kolodner, P.; Krupenkin, T. N. *Langmuir* **2008**, *24*, 9–14.
(12) Cao, L.; Hu, H.-H.; Gao, D. *Langmuir* **2007**, *23*, 4310–4314.
(13) Tuteja, A.; Choi, W.; Ma, M.; Mabry, J. M.; Mazzella, S. A.; Rutledge, G. C.; McKinley, G. H.; Cohen, R. E. *Science* **2007**, *318*, 1618–1622.
(14) Tuteja, A.; Choi, W.; Mabry, J. M.; McKinley, G. H.; Cohen, R. E. *Proc. Natl. Acad. Sci.* **2008**, *105*, 18200–18205.

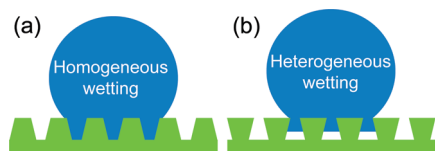


Figure 1. Schematic diagrams of liquid droplets on microstructured surfaces under (a) the homogeneous (Wenzel) regime and (b) the heterogeneous (Cassie–Baxter) regime.

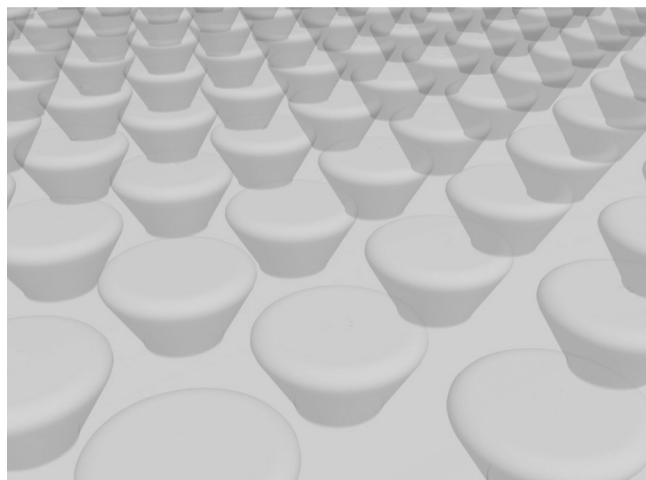


Figure 2. Schematic illustration of a PDMS trapezoids surface.

surfaces. In particular, the microstructures with overhangs illustrated in Figure 1b demonstrate the metastable Cassie–Baxter state, as the net force is generated in the upward direction to support a liquid droplet.^{12,14} These types of overhang structures have advantages in creating a superhydrophobic surface with a hydrophilic material^{12,15,16} and realizing an oleophobic surface.^{14,17} The authors recently reported a superhydrophobic surface comprised of overhang structures of inverted truncated cones¹⁷ (i.e., inverse-trapezoids), as illustrated in Figure 2. Those microstructures were fabricated with a flexible and transparent polymer (polydimethylsiloxane, PDMS). Transmittance analysis and optical images of this superhydrophobic surface can be easily found in our previous publication.¹⁷ Including the sidewall angle, the geometrical parameters of the inverse-trapezoidal microstructures (hereafter referred to as “PDMS trapezoids”) are explicitly controllable by the novel fabrication process.¹⁸ To enhance the hydrophobic property and the transmittance, a Teflon layer was coated onto the PDMS trapezoids¹⁷ to combine physical and chemical modifications, as in previous researches.^{19–21}

The present paper discusses the impact of the design parameters on the hydrophobicity of PDMS trapezoids surfaces with the aid of thermodynamic analyses. Although superhydrophobicity and oleophobicity were experimentally demonstrated¹⁷ on a Teflon-coated PDMS trapezoids surface, analytical modeling is necessary to optimize the hydrophobic property and to understand the underlying physics comprehensively through engineering of the shape of PDMS

trapezoids array. Through a Gibbs free energy analysis and estimation of the contact angles, we claim that the robust superhydrophobicity on the fabricated Teflon-coated PDMS trapezoids surface is achieved. Deeper analysis by an impinging droplet test supports the contention of robust superhydrophobicity. Finally, the Gibbs free energy analysis is expanded for different heights and side angles. The results show good agreement with the measured contact angle data.

2. Theory

2.1. Thermodynamic Analysis of the Wetting State. From a thermodynamic perspective, one of the two states of the Wenzel state and/or the Cassie–Baxter state has the local minimum of the energy, whereas the other has the global minimum of the energy, which is energetically more favorable. However, depending on the droplet formation method, a liquid droplet on a rough surface can stay on a metastable point^{11–14} that is provided by the local energy minimum state.

When liquid spreads over a surface, the original interface is destroyed. This can lead to a gain or loss in the overall free energy of the system because surface tension must be overcome. This process will continue until the minimum energy level is reached. If the total energy level is continuously reduced as the wetting process advances, the rough surface will tend to be fully wetted. On the other hand, a composite interface can be obtained if the total energy meets the minimum value before the liquid reaches the bottom of the surface. Marmur²² showed that the stability of a composite interface can be predicted by computing the Gibbs free energy (G), as given by

$$G = \gamma_{sl}A_{sl} + \gamma_{la}A_{la} + \gamma_{sa}A_{sa} \quad (3)$$

where γ is the interfacial surface tension, A is the interfacial area, and the subscripts s, l, and a denote the solid, liquid, and air, respectively.

Marmur also claimed that the apparent contact angle of the structured surface can be estimated by an analysis of the Gibbs free energy. Recently, Tuteja et al.¹⁴ referred to Marmur’s work and used *Matlab* (Mathworks Inc.) to compute the Gibbs free energy density (G^*) of their structures and drew three-dimensional graphs of G^* , which is the Gibbs free energy normalized by the original surface area of a liquid droplet. The same method is used here to estimate the apparent contact angles of a fresh (Teflon-uncoated) PDMS trapezoids surface and a Teflon-coated PDMS trapezoids surface. Numerically, G^* is calculated as²²

$$G^* = (2 - 3 \cos \theta_{app} + \cos^3 \theta_{app})^{-2/3} [2 - 2 \cos \theta_{app} - \sin^2 \theta_{app} (r_f \cos \theta_{FLAT} + f - 1)] \quad (4)$$

where θ_{app} is the apparent contact angle, θ_{FLAT} is the apparent contact angle on a flat surface made of the same material, f is the area fraction of the solid region at the liquid–air interface, and r_f is the roughness ratio of the wetted area. Apparent contact angles in the Wenzel regime and the Cassie–Baxter regime can be defined with the minimal G^* under a fully wetted and a partially wetted condition, respectively. Section 3.2 details the procedure used to extract each contact angle.

2.2. Robustness of Superhydrophobic Surfaces. Many previous studies^{11,12,23–32} have reported a transition of the wetting

- (15) Marmur, A. *Langmuir* **2008**, *24*(14), 7573–7579.
- (16) Liu, J.-L.; Feng, X.-Q.; Wang, G.; Yu, S.-W. *J. Phys.: Condens. Matter* **2007**, *19*, 356002.
- (17) Im, M.; Im, H.; Lee, J.-H.; Yoon, J.-B.; Choi, Y.-K. *Soft Matter* **2010**, *6*(7), 1401–1404.
- (18) Lee, J.-H.; Choi, W.-S.; Lee, K.-H.; Yoon, J.-B. *J. Micromech. Microeng.* **2008**, *18*, 125015.
- (19) Balu, B.; Breedveld, V.; Hess, D. W. *Langmuir* **2008**, *24*, 4785–4790.
- (20) Dhindsa, M. S.; Smith, N. R.; Heikenfeld, J.; Rack, P. D. *Langmuir* **2006**, *22*, 9030–9034.
- (21) Krupenkin, T. N.; Taylor, J. A.; Schneider, T. M.; Yang, S. *Langmuir* **2004**, *20*, 3824–3827.
- (22) Marmur, A. *Langmuir* **2003**, *19*, 8343–8348.
- (23) Bico, J.; Marzolin, C.; Quéré, D. *Europhys. Lett.* **1999**, *47*(2), 220–226.
- (24) Patankar, N. A. *Langmuir* **2003**, *19*, 1249–1253.
- (25) Barbieri, L.; Wagner, E.; Hoffmann, P. *Langmuir* **2007**, *23*, 1723–1734.
- (26) Sbragaglia, M.; Peters, A. M.; Pirat, C.; Borkent, B. M.; Lammertink, R. G. H.; Wessling, M.; Lohse, D. *Phys. Rev. Lett.* **2007**, *99*(15), 156001.
- (27) Bartolo, D.; Bouamrine, F.; Verneuil, E.; Buguin, A.; Silberzan, P.; Moulinet, S. *Europhys. Lett.* **2006**, *74*(2), 299–305.
- (28) Patankar, N. A. *Langmuir* **2004**, *20*, 7097–7102.
- (29) Brunet, P.; Lapierre, F.; Thomay, V.; Coffinier, Y.; Boukherroub, R. *Langmuir* **2008**, *24*(19), 11203–11208.
- (30) Jopp, J.; Grull, H.; Yerushalmi-Rozen, R. *Langmuir* **2004**, *20*(23), 10015–10019.
- (31) Dorrier, C.; Rühe, J. *Langmuir* **2007**, *23*(7), 3820–3824.
- (32) Bahadur, V.; Garimella, S. V. *Langmuir* **2009**, *25*(8), 4815–4820.

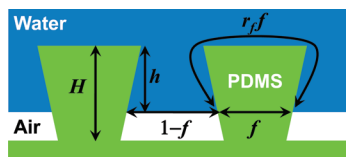


Figure 3. Schematic illustration that shows the parameters used in the calculation of the Gibbs free energy density; the area fraction of the solid region at the liquid–air interface (f), the roughness ratio of the wetted region (r_f), the sagging height (h), and the height of the PDMS trapezoids (H).

behavior from the Cassie–Baxter state to the Wenzel state, and vice versa. Contact angle changes from one state to the other state can usually be induced by external disturbances such as pressure,²³ motion,²⁴ and the presence of an electrical field,¹¹ which can supply energy to the system so as to overcome the energy barrier between the global and local energy minima. If the contact angles in two wetting states are different, a rough surface may lose its superhydrophobicity as a result of external disturbances. This can also occur spontaneously.²⁶

Patankar proposed the concept of a robust and stable superhydrophobic surface having the same apparent contact angles in both the Wenzel and the Cassie–Baxter states ($\theta_W = \theta_{CB}$),²⁴ and some attempts have been made to realize this concept.^{25,33} However, there are no reports pertaining to the realization of a robust superhydrophobic surface that shows nearly identical apparent contact angles in both wetting states. Alternatively, a robust superhydrophobic surface can be realized when the apparent contact angle does not change due to the impossible existence of the Wenzel state. On microstructured surfaces, few researchers have reported robust superhydrophobicity only in Cassie–Baxter states which cannot be changed to the Wenzel state.^{9,14,25,31,32}

In this article, a fabricated Teflon-coated PDMS trapezoids surface is analyzed thermodynamically through the use of the Gibbs free energy density to observe dependencies on various design parameters. With the aid of an additional Teflon coating process, the PDMS trapezoids surface shows robust superhydrophobicity with a stable Cassie–Baxter state and automatic transition from the Wenzel state to the Cassie–Baxter state in the Gibbs free energy density analysis. Moreover, for the first time, nearly equal ($\Delta\theta = \theta_W - \theta_{CB} \approx 1^\circ$) apparent contact angles in both wetting states are estimated through thermodynamic analyses of the precisely engineered dimensions of the PDMS trapezoids. Robust superhydrophobicity is supported by water droplet impinging experiments.

3. Results and Discussions

3.1. Derivation of the Solid Area Fraction (f) and the Roughness Ratio (r_f) as a Function of the Sagging Height (h) in PDMS Trapezoids. An appropriate analytical model of PDMS trapezoids is essential for a comprehensive understanding of these trapezoids and for optimization of their geometric parameters. For a more precise estimation of the apparent contact angles in the Wenzel and the Cassie–Baxter states, the liquid contacting area fraction (f) and the roughness factor (r_f) of a PDMS trapezoids surface are calculated as a function of the sagging height (h), as described in Figure 3. In detail, h is defined as the distance between the liquid–air interface and the top of the rough surface, and f is the ratio of the solid area to the total area of the projected plane from the top. Here, the solid area is the fraction occluded by liquid in the cross-section on the same plane with the liquid meniscus. Lastly, r_f is the ratio

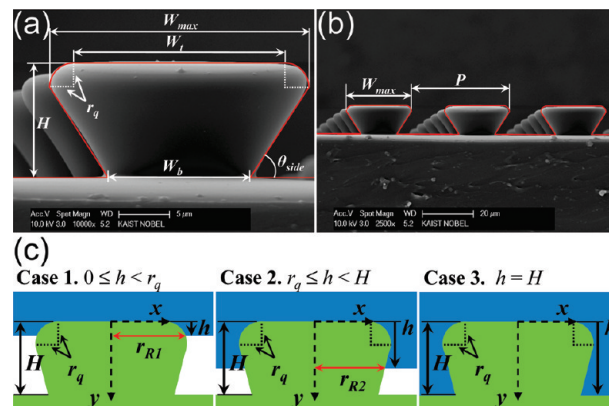


Figure 4. (a and b) SEM images of the PDMS trapezoids.¹⁵ Reproduced with permission of The Royal Society of Chemistry. The parameters used in the developed model, and an approximated profile of a PDMS trapezoid (red solid line). The rounded region of the PDMS trapezoid is assumed to be a quarter of a circle with a radius of $3.6 \mu\text{m}$. The maximum width of the PDMS trapezoids (W_{max}) is used to describe the effect of roundness, because the width at the end of a rounded region is longer than the width at the top (W_t). The trapezoid is modeled with a linear slope of $\tan \theta_{\text{side}}$ below the rounded region. (c) Schematics exhibit various parameters to derive f and r_f as a function of h . Three wetting cases are assumed for accurate calculations. Case 1: When the liquid–air interface line is positioned at the rounded region of a PDMS trapezoid ($0 \leq h < r_q$). Case 2: When the liquid–air interface line is formed at the linear region ($r_q \leq h < H$). Case 3: When the surface is fully wetted ($h = H$).

of the actual wetted area to the solid area that is occluded by liquid.

Although an ideal trapezoid pillar had been modeled and analyzed in terms of two-dimensional surface energy,¹⁶ this previous work cannot be applied to our fabricated three-dimensional microstructures because the top surface of a PDMS trapezoid is not completely flat. The rounded profile at the upper corners should be considered, as shown in Figure 4a, for an accurate computation of f and r_f that are critical in estimation of contact angles. In the following equations, the rounded region is approximated to be a quarter of a circle with a radius of r_q . Subsequently, it becomes possible to derive f and r_f from an approximated profile that is similar to the actual profile of a PDMS trapezoid. From the scanning electron microscope (SEM) images in Figure 4, panels a and b, r_q is determined to be $3.6 \mu\text{m}$. Given that the size of r_q is suitably controlled by the exposure condition during the fabrication process, r_q is uniform and reproducible under the same exposure conditions. Hence, this value is used in the subsequent analysis.

The cross-section of a PDMS trapezoid in parallel with the substrate surface is always a circle. In this case, the overall shape of the PDMS trapezoid is an inverted structure of a truncated cone. Therefore, if the radius of the PDMS trapezoid on the same plane with the liquid meniscus is calculated at any arbitrary vertical position, f and r_f can be calculated as well. As depicted in Figure 4c, we categorize three wetting cases differentiated by the sagging height (h) because the liquid meniscus can stay on the sidewall of the PDMS trapezoid at (1) the rounded profile region, (2) the linear profile region, or (3) the bottom. Figure 4c also illustrates the parameters used in the calculation of f and r_f . The details of the computations in the three cases are given below.

(33) He, B.; Patankar, N. A.; Lee, J. *Langmuir* **2003**, *19*, 4999–5003.

Case 1. When $0 \leq h < r_q$ (the Liquid Meniscus at the Rounded Profile Region of the Sidewall). The first step is to derive the radius of the cross-section (r_{R1}) of the PDMS trapezoid on the sagging plane, which is in parallel with the substrate surface, when the sagging stops at the rounded profile region. This radius is calculated through the sum of the half of the top width (W_t) of the trapezoid and the additional width that originates from the rounded profile

$$r_{R1} = \frac{W_t}{2} + \sqrt{r_q^2 - (y - r_q)^2} \quad (5)$$

Subsequently, f is calculated as

$$f = \frac{\pi(r_{R1}|_{y=h})^2}{P^2} \quad (6)$$

where P is the pitch between adjacent PDMS trapezoids. The numerator in eq 6 is the solid area in the cross-section of the PDMS trapezoid on the same plane with the liquid meniscus. The denominator is the area of a unit cell of the PDMS trapezoids array, which is equal to the area of a square having four sides as the pitch of the PDMS trapezoids.

The second step is to calculate r_f

$$\begin{aligned} r_f &= \frac{\pi\left(\frac{W_t}{2}\right)^2 + \int_0^h 2\pi r_{R1} dy}{\pi(r_{R1}|_{y=h})^2} \\ &= \frac{\pi\left(\frac{W_t}{2}\right)^2 + \int_0^h 2\pi \left[\left(\frac{W_t}{2}\right) + \sqrt{r_q^2 - (y - r_q)^2} \right] dy}{\pi(r_{R1}|_{y=h})^2} \\ &= \frac{\pi\left(\frac{W_t}{2}\right)^2 + 2\pi\left(\frac{W_t}{2}\right)h + 2\pi r_q h}{\pi(r_{R1}|_{y=h})^2} \\ &= \frac{\left(\frac{W_t}{2}\right)^2 + W_t h + 2r_q h}{(r_{R1}|_{y=h})^2} \quad (7) \end{aligned}$$

From the above equation, the numerator is the area which is wetted in the PDMS trapezoids when the liquid meniscus stays on h . It is calculated through the sum of the top area and the side area which is wetted. The denominator is the area which is identical to the value of the numerator in f .

Case 2. When $r_q \leq h < H$ (the Liquid Meniscus at the Linear Profile Region of the Sidewall). Similarly, f and r_f are derived when the liquid meniscus lies at the linear profile region of the sidewall. In this case, the radius of the cross-section (r_{R2}) of the PDMS trapezoid on the sagging plane is calculated by

$$r_{R2} = \frac{\left(\frac{W_b}{2}\right) - \left(\frac{W_{\max}}{2}\right)}{H - r_q} (y - r_q) + \frac{W_{\max}}{2} \quad (8)$$

In the above equation, r_{R2} has its maximum value when it is at the boundary ($y = r_q$) between the rounded profile region and the linear region. In this case, r_{R2} is identical to $W_{\max}/2$. When y increases, r_{R2} decreases linearly.

Likewise, f and r_f can then be derived

$$f = \frac{\pi(r_{R2}|_{y=h})^2}{P^2} \quad (9)$$

$$\begin{aligned} r_f &= \frac{\pi\left(\frac{W_t}{2}\right)^2 + 2\pi\left(\frac{W_t}{2}\right)r_q + 2\pi r_q^2 + \int_{r_q}^h 2\pi r_{R2} dy}{\pi(r_{R2}|_{y=h})^2} \\ &= \left\{ \pi \left[\left(\frac{W_t}{2}\right)^2 + 2\left(\frac{W_t}{2}\right)r_q + 2r_q^2 + \frac{\left(\frac{W_b}{2}\right) - \left(\frac{W_{\max}}{2}\right)}{H - r_q} (h - r_q)^2 \right. \right. \\ &\quad \left. \left. + 2\left(\frac{W_{\max}}{2}\right)(h - r_q) \right] \right\} / \left\{ \pi(r_{R2}|_{y=h})^2 \right\} \\ &= \frac{\left(\frac{W_t}{2}\right)^2 + W_t r_q + 2r_q^2 + \frac{\left(\frac{W_b}{2}\right) - \left(\frac{W_{\max}}{2}\right)}{H - r_q} (h - r_q)^2 + W_{\max}(h - r_q)}{(r_{R2}|_{y=h})^2} \quad (10) \end{aligned}$$

Case 3. When $h = H$ (the Liquid Touches the Bottom). When the liquid touches the bottom of a PDMS trapezoid due to sagging, f equals 1. In this case, r_f is calculated by

$$\begin{aligned} r_f &= \frac{\left[P^2 - \pi\left(\frac{W_b}{2}\right)^2 \right] + \pi\left(\frac{W_t}{2}\right)^2 + \left[\int_0^{r_q} 2\pi r_{R1} dy + \int_{r_q}^H 2\pi r_{R2} dy \right]}{P^2} \\ &= 1 + \left\{ \pi \left[\left(\frac{W_t}{2}\right)^2 - \left(\frac{W_b}{2}\right)^2 + W_t r_q + 2r_q^2 \right. \right. \\ &\quad \left. \left. + \left(\frac{W_b}{2} - \frac{W_{\max}}{2}\right)(H - r_q) + W_{\max}(H - r_q) \right] \right\} / \{ P^2 \} \quad (11) \end{aligned}$$

In the first row of the above equation, the numerator is the wetted area in the unit cell of the PDMS trapezoids when the liquid meniscus touches its bottom. It is composed of three terms: the wetted area on the bottom, on the top, and on the sidewall in the unit cell of the PDMS trapezoids. The denominator is the projected area of a unit cell of the PDMS trapezoids array.

3.2. Contact Angle Analysis by Calculation of the Gibbs Free Energy Density. In order to find the theoretical apparent contact angle of the PDMS trapezoids surface, the Gibbs free energy density (G^*) is calculated by eq 4. By plugging the calculated values of f and r_f in the previous section into eq 4, G^* becomes a function of two independent variables, i.e., h and θ_{app} . For unknown values of h and θ_{app} , G^* is computed for a temporary apparent contact angle (θ_t) varying in the range of $0^\circ < \theta_t < 180^\circ$ for θ_{app} , with h varying in the range of $0 \leq h \leq H$.¹⁴ We developed our own *Matlab* code to compute complex equations and plot the three-dimensional graphs of G^* , as shown in Figure 5. The apparent contact angle in the Cassie–Baxter state (θ_{app}^{CB}) is estimated to be the value of θ_t which minimizes G^* in the range of $0 \leq h < H$.¹⁴ In contrast, the apparent contact angle in the Wenzel state (θ_{app}^W) has the value of θ_t , which minimizes G^* in a fully wetted condition (i.e., $h = H$).¹⁴

Figure 5 shows the calculated results of G^* for a droplet of deionized water ($\gamma_{la} = 72$ mN/m) on a PDMS trapezoids surface before and after it receives a Teflon coating. As shown in Figures 5, panels a and b, a fresh PDMS trapezoids surface

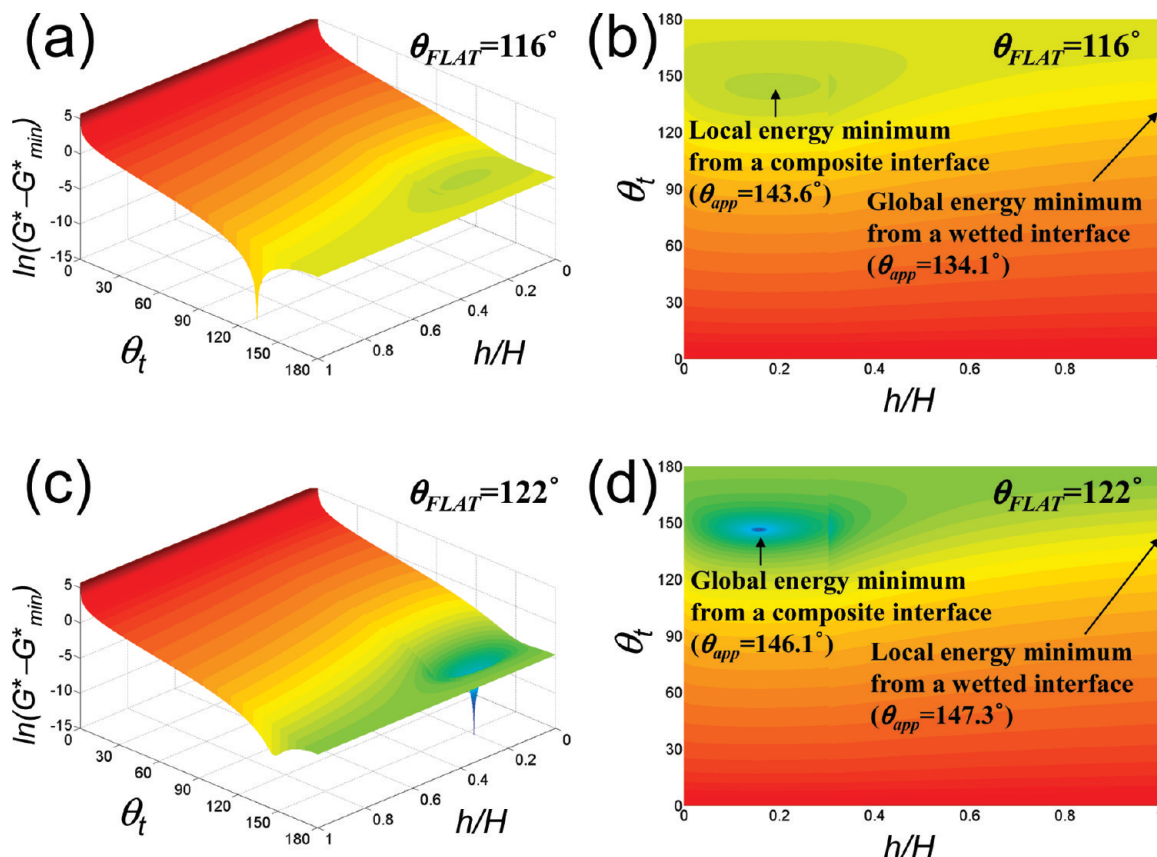


Figure 5. PDMS trapezoids of $H = 11.9 \mu\text{m}$, $\theta_{\text{side}} = 56^\circ$, and $P = 40 \mu\text{m}$. (a) The change in the Gibbs free energy density (G^*) of a fresh PDMS trapezoids surface ($\theta_{\text{FLAT}} = 116^\circ$) as a function of θ_t (temporal apparent contact angle) and h/H (portion of sagging height). Here, G_{min}^* is the Gibbs free energy density at the global minimum. The fresh PDMS trapezoids surface has two energy minima when $h/H = 0.18$ ($h = 2.1 \mu\text{m}$) and $h/H = 1$, which correspond to a composite interface and a fully wetted interface, respectively. The global energy minimum is observed at $h/H = 1$. (b) Top view of the energy diagram, as shown in (a). (c) The change in the Gibbs free energy density (G^*) of a Teflon-coated PDMS trapezoids surface ($\theta_{\text{FLAT}} = 122^\circ$) as a function of θ_t and h/H . The Teflon-coated PDMS trapezoids surface has two energy minima when $h/H = 0.16$ ($h = 1.9 \mu\text{m}$) and $h/H = 1$, which correspond to a composite interface and a fully wetted interface, respectively. The global energy minimum is observed at $h/H = 0.16$. (d) Top view of the energy diagram, as shown in (c).

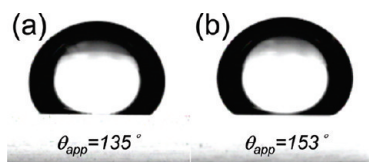


Figure 6. Contact angles of deionized water on the fabricated PDMS trapezoids (a) before coating with Teflon and (b) after coating with Teflon.

($\theta_{\text{FLAT}} = 116^\circ$) has two Gibbs free energy minima when $h/H = 0.18$ ($h = 2.1 \mu\text{m}$) and $h/H = 1$, which correspond to a partially wetted (composite) interface and a fully wetted interface, respectively. The former is the local energy minimum which corresponds to the metastable Cassie–Baxter state ($\theta_{\text{app}}^{\text{CB}} = 143.6^\circ$), and the latter is the global energy minimum which corresponds to the stable Wenzel state ($\theta_{\text{app}}^{\text{W}} = 134.1^\circ$). In the case of fresh PDMS trapezoids, the Wenzel state is more thermodynamically favorable and a noticeable discrepancy exists between the two contact angles. This indicates that the contact angle may be significantly changed by some disturbances due to the transition from the Cassie–Baxter state to the Wenzel state if the droplet is initially in the metastable Cassie–Baxter state.

However, as shown in Figures 5, panels c and d, the results for a Teflon-coated PDMS trapezoids surface ($\theta_{\text{FLAT}} = 122^\circ$) are entirely different. As with the fresh PDMS trapezoids surface,

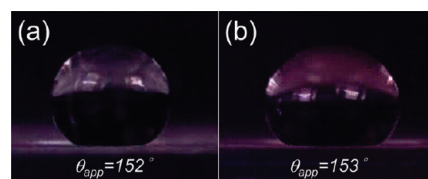


Figure 7. (a and b) Contact angles of deionized water on a fabricated Teflon-coated PDMS trapezoids surface after water droplet impinging tests.

the Teflon-coated PDMS trapezoids surface has two minima when $h/H = 0.16$ ($h = 1.9 \mu\text{m}$) and $h/H = 1$. In this case, however, the former is the global energy minimum which corresponds to a composite interface ($\theta_{\text{app}}^{\text{CB}} = 146.1^\circ$), while the latter is the local energy minimum which corresponds to a fully wetted interface ($\theta_{\text{app}}^{\text{W}} = 147.3^\circ$). It is worthwhile to note that the Cassie–Baxter state becomes energetically more favorable than the Wenzel state with an additional Teflon coating. Moreover, the contact angle difference becomes much smaller compared to the difference with a fresh PDMS trapezoids surface. The reason for the difference between before and after the Teflon coating is simply the dissimilarity between θ_{FLAT} : $\theta_{\text{FLAT,PDMS}} = 116^\circ$ and $\theta_{\text{FLAT,Teflon}} = 122^\circ$.

Figure 5d clearly shows that the Cassie–Baxter drop has a lower energy with a lower contact angle compared to these aspects

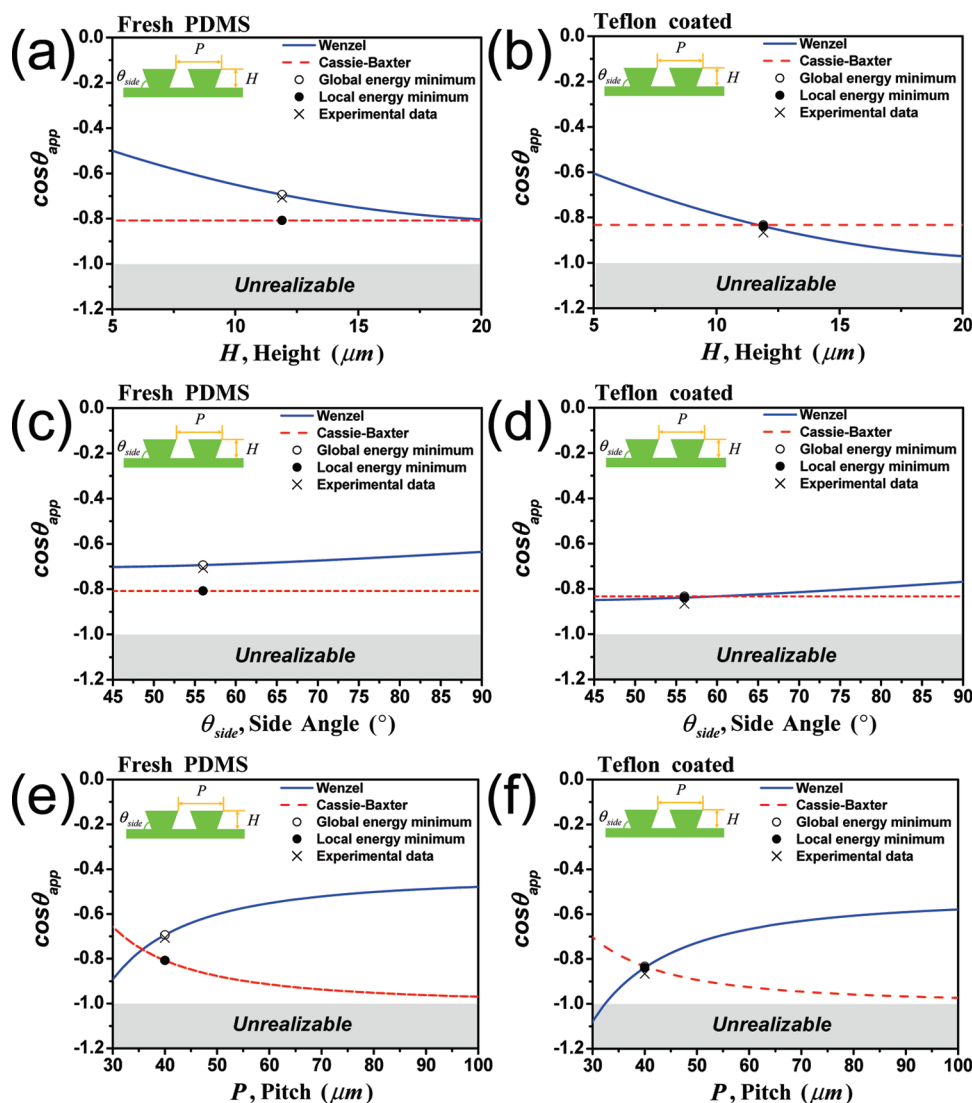


Figure 8. Dependency of the apparent contact angles on various design parameters (H , θ_{side} , and P) of a fresh PDMS trapezoids surface ($\theta_{\text{FLAT}} = 116^\circ$) and a Teflon-coated PDMS trapezoids surface ($\theta_{\text{FLAT}} = 122^\circ$) according to the Wenzel and the Cassie–Baxter equation. Calculated apparent contact angles for (a) a fresh PDMS trapezoids surface and (b) a Teflon-coated PDMS trapezoids surface as a function of H (with $\theta_{\text{side}} = 56^\circ$, $P = 40 \mu\text{m}$, and $W_t = 26 \mu\text{m}$), and measured contact angles (marked with “x”) of the fabricated surface at $H = 11.9 \mu\text{m}$. The calculated apparent contact angles for (c) a fresh PDMS trapezoids surface and (d) a Teflon-coated PDMS trapezoids surface as a function of θ_{side} (with $H = 11.9 \mu\text{m}$, $P = 40 \mu\text{m}$, and $W_t = 26 \mu\text{m}$), and measured contact angles (marked with “x”) of the fabricated surface at $\theta_{\text{side}} = 56^\circ$. The calculated apparent contact angles for (e) a fresh PDMS trapezoids surface and (f) a Teflon-coated PDMS trapezoids surface as a function of P (with $H = 11.9 \mu\text{m}$, $\theta_{\text{side}} = 56^\circ$, and $W_t = 26 \mu\text{m}$), and measured contact angles (marked with “x”) of the fabricated surface at $P = 40 \mu\text{m}$. Global and local energy minima shown in the figures are attained by calculating the Gibbs free energy density.

of the Wenzel drop. This thermodynamical analysis implies that the Cassie–Baxter state is more favorable and stable for any droplet on a Teflon-coated PDMS trapezoids surface. Figure 5d also shows a monotonous decrease along the path from the wetted interface to the composite interface. In addition to the stability of the composite interface, this also assures that a droplet undergoes a zero energy barrier in the transition from the fully wetted Wenzel state to the Cassie–Baxter state. Like the Teflon-coated PDMS trapezoids, an energy barrier may not exist between two wetting states for a certain surface geometry.²⁸ In this case, the droplet would always be triggered to enter the Cassie–Baxter state spontaneously, even if the droplet is initially in the metastable Wenzel region due to a certain condition, such as gentle placement.

It is believed that θ_{app} in the equilibrium state can be determined in the condition where the value of Gibbs free energy density has its global minimum. In this manner, we conclude that

a fresh PDMS trapezoids surface theoretically has a θ_{app} value of 134.1° and that a Teflon-coated PDMS trapezoids surface has a θ_{app} value of 146.1° . These estimated values are close to the measured data in Figure 6. Furthermore, with Teflon-coated PDMS trapezoids, it is notable again that a spontaneous transition to the Cassie–Baxter state is expected and that the contact angles in both wetting states become very similar. This robust superhydrophobicity of the Teflon-coated PDMS trapezoids surface is discussed in the following section.

3.3. Robustness Test by an Impinging Water Droplet. To confirm the robustness of superhydrophobic surfaces, researchers made a transition of the wetting state from Cassie–Baxter to Wenzel by pushing droplets,^{9,23,34} or by dropping droplets from a certain height.³³ In particular, He et al. analyzed the robustness of the superhydrophobicity of micropillared surfaces by comparing

(34) Lafuma, A.; Quéré, D. *Nat. Mater.* **2003**, *2*, 457–460.

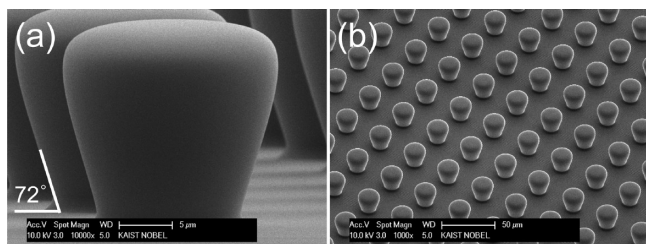


Figure 9. SEM images of fabricated PDMS trapezoids with $H = 20 \mu\text{m}$, $\theta_{\text{side}} = 72^\circ$, and $W_t = 21 \mu\text{m}$, $P = 40 \mu\text{m}$; (a) Cross-sectional view of a single trapezoid and (b) tilted view of a PDMS trapezoids array.

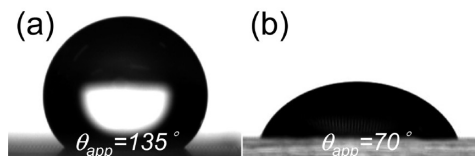


Figure 10. (a) Contact angle of a methanol ($\gamma_{\text{la}} = 22.7 \text{ mN/m}$) droplet on the Teflon-coated PDMS trapezoids of $H = 11.9 \mu\text{m}$, $\theta_{\text{side}} = 56^\circ$, and $P = 40 \mu\text{m}$ as shown in Figure 4.¹⁵ Reproduced with permission of The Royal Society of Chemistry. (b) Contact angle of a methanol droplet on the Teflon-coated PDMS trapezoids of with $H = 20 \mu\text{m}$, $\theta_{\text{side}} = 72^\circ$, and $P = 40 \mu\text{m}$ as shown in Figure 9.

two droplet contact angles after droplets were gently deposited and deposited from a certain height.³³ However, in their experiments, they could achieve neither a zero contact angle difference nor a value close to zero.

Unless external energy is applied to a system of a liquid droplet and a Teflon-coated PDMS trapezoids surface, a transition in the wetting behavior of a droplet is not allowed due to the lack of energy to overcome the energy barrier between two wetting states. To check the possibility of a transition from the Cassie–Baxter state at the global energy minimum to the Wenzel state at the local energy minimum on a Teflon-coated PDMS trapezoids surface, kinetic energy was supplied to the system by dropping a water droplet from a certain height. Through the release of a deionized water droplet from a height of 3.2 cm, an impacting velocity (V_{impact}) of 79.2 cm/sec was obtained.¹⁷ The motions of free falling water drops of which the radius is 1 mm were recorded with a high-speed camera (Phantom v5.0, Vision Research, Inc.) at a frame rate of 4000 frames/sec. After the impact, the water droplets completely rebounded on the Teflon-coated PDMS trapezoids surface, whereas a water droplet became stuck on a Teflon-coated flat PDMS surface.¹⁷ This result can be interpreted by the fact that small contact angle hysteresis³⁵ is attained on the superhydrophobic Teflon-coated PDMS trapezoids surface. Contact angle hysteresis of a PDMS trapezoids surface is decreased to be 18° by coating of Teflon, whereas it is 44° without Teflon.¹⁷ Therefore, the water droplet is considered to be in the Cassie–Baxter state because a Wenzel drop generally has large contact angle hysteresis.⁹

Figure 7 shows droplets and their contact angles after settlement followed by a free falling test from a height of 3.2 cm. The contact angles were nearly identical (e.g., the contact angle differences were within 1° in several experiments) to those shown in Figure 6b, which were gently deposited on a Teflon-coated PDMS

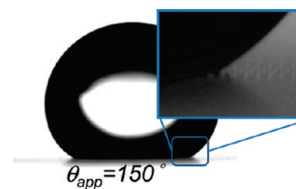


Figure 11. Contact angle of deionized water on the Teflon-coated PDMS trapezoids shown in Figure 9. Inset: Close-up view of the location near the contact line. The Cassie–Baxter state is confirmed by the microstructures shown underneath the water droplet.

trapezoids surface. This verifies the robustness of the proposed superhydrophobic surface.

As described in the previous section and as shown in Figure 5d, the Gibbs free energy density is monotonously increased from the global minimum of G^* (the Cassie–Baxter state) to the local minimum of G^* (the Wenzel state). The energy difference between these two states is equivalent to the energy barrier seen from the Cassie–Baxter state at the global energy minimum on the Teflon-coated PDMS trapezoids surface. It should be noted that G^* is a normalized and dimensionless value.²² Therefore, it is necessary to rewrite the Gibbs free energy formula by considering the relevant dimensions, as follows:²²

$$G = \gamma_{\text{la}} \pi^{1/3} (3V)^{2/3} G^* = \gamma_{\text{la}} \pi^{1/3} (3V)^{2/3} (2 - 3 \cos \theta_{\text{app}} + \cos^3 \theta_{\text{app}})^{-2/3} [2 - 2 \cos \theta_{\text{app}} - \sin^2 \theta_{\text{app}} (r_f f \cos \theta_{\text{FLAT}} + f - 1)] \quad (12)$$

In this equation, γ_{la} is the liquid–air surface tension and V is the volume of the liquid. In our experiments, $\gamma_{\text{la}} = 72 \text{ mN/m}$ (deionized water at 25°C), and $V = 4.19 \mu\text{L}$ (estimated volume of the water droplet used in the impinging test). The energy difference is defined as $\Delta E = E_{\text{W}} - E_{\text{CB}}$, where E_{W} is the energy in the Wenzel state and E_{CB} is the energy in the Cassie–Baxter state. The calculated value of ΔE is 0.38 nJ according to eq 12.

The kinetic energy ($E = (1/2)MV_{\text{impact}}^2 = 1.307 \mu\text{J}$) of the impinging water droplet ($V = 4.19 \mu\text{L}$ corresponding to $M = 4.19 \text{ mg}$; $V_{\text{impact}} = 79.2 \text{ cm/s}$) is three thousand times larger than the energy difference (0.38 nJ) between the Wenzel and the Cassie–Baxter state. Hence, it is believed that some fraction of the kinetic energy can contribute to overcoming the energy barrier during a transition from the Cassie–Baxter to the Wenzel state if the droplet is initially in the Cassie–Baxter state. However, large contact angle hysteresis, which is a general characteristic of a Wenzel drop, was not observed here. In consequence, it is more evident that the water droplet returns automatically to the Cassie–Baxter regime in order to satisfy the thermodynamical stability at the lowest energy,⁹ even after the impinging test.

In general, a transition from the Cassie–Baxter state to the Wenzel state is regarded to be irreversible because the Wenzel state has the global energy minimum in most cases.³⁶ However, when the Cassie–Baxter state is energetically more favorable than the Wenzel state, the opposite transition is also possible according to the literature.³¹

The breakthrough pressure,^{13,14} which is defined as the required pressure for the transition from the Cassie–Baxter to the Wenzel state, is effectively infinite on this very stable superhydrophobic surface as the apparent contact angles are nearly identical in both states and because the Wenzel drop always transitions to the Cassie–Baxter drop. Particularly, due to this

(35) Wang, Z.; Lopez, C.; Hirs, A.; Koratkar, N. *Appl. Phys. Lett.* **2007**, *91*(2), 023105.

(36) Dorrier, C.; R  he, J. *Soft Matter* **2009**, *5*(1), 51–61.

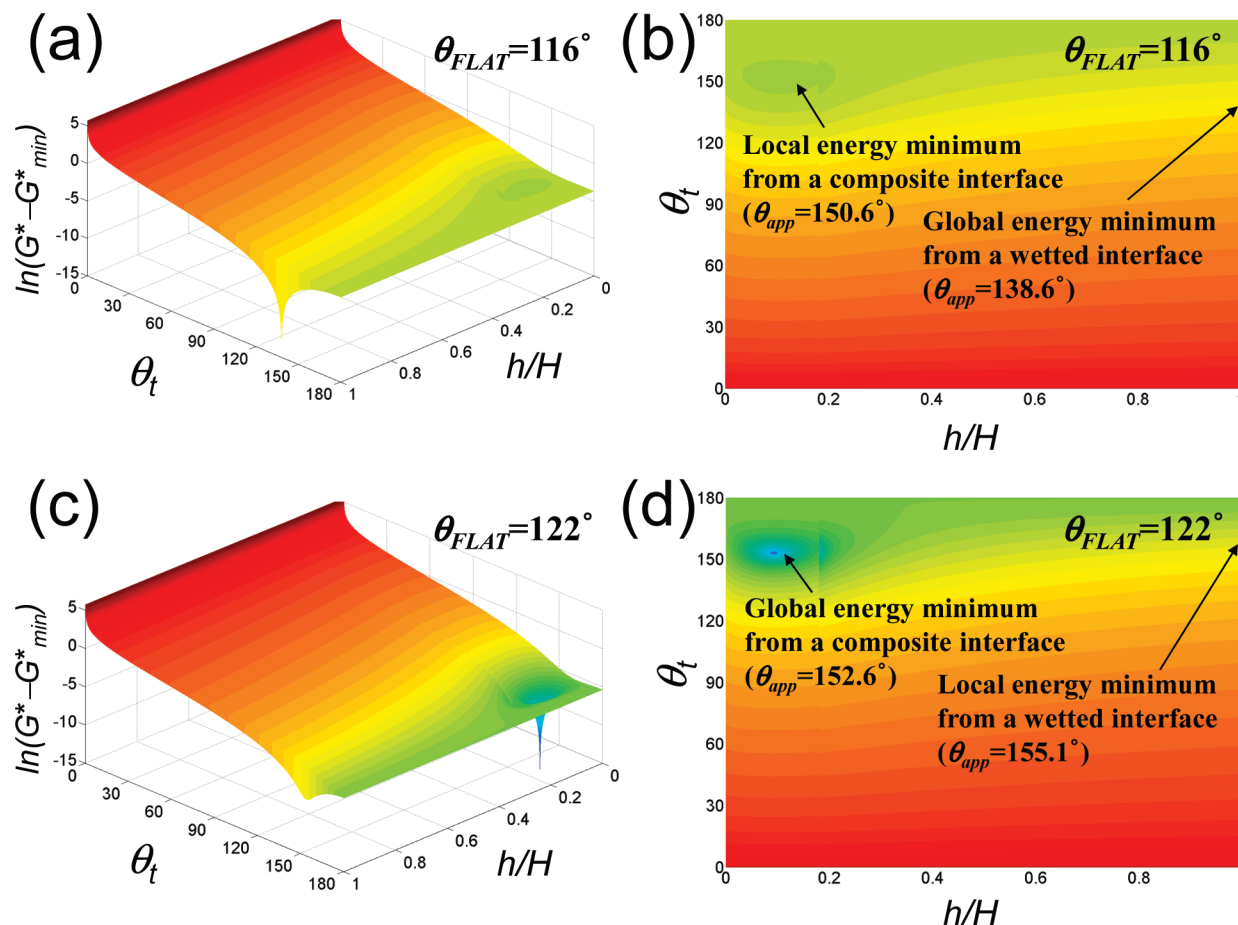


Figure 12. With the geometry of $H = 20 \mu\text{m}$, $\theta_{\text{side}} = 72^\circ$, and $P = 40 \mu\text{m}$. (a) The change in the Gibbs free energy density (G^*) of a fresh PDMS trapezoids surface ($\theta_{\text{FLAT}} = 116^\circ$) as a function of θ_t (temporal apparent contact angle) and h/H (portion of sagging height). Here, G_{min}^* is the Gibbs free energy density at the global minimum. The fresh PDMS trapezoids surface has two energy minima when $h/H = 0.105$ ($h = 2.1 \mu\text{m}$) and $h/H = 1$, which correspond to a composite interface and a fully wetted interface, respectively. The global energy minimum is observed at $h/H = 1$. (b) Top view of the energy diagram, as shown in (a). (c) The change in the Gibbs free energy density (G^*) of a Teflon-coated PDMS trapezoids surface ($\theta_{\text{FLAT}} = 122^\circ$) as a function of θ_t and h/H . The Teflon-coated PDMS trapezoids surface has two energy minima when $h/H = 0.095$ ($h = 1.9 \mu\text{m}$) and $h/H = 1$, which correspond to a composite interface and a fully wetted interface, respectively. The global energy minimum is observed at $h/H = 0.095$. (d) Top view of the energy diagram, as shown in (c).

unique feature, the fabricated Teflon-coated PDMS trapezoids surface is expected to be used under a high-pressure environment, such as a diving suit or a submarine application. Moreover, water droplets will likely roll off of a diving or swimming suit made of the Teflon-coated PDMS trapezoids after the wearer gets out of the water.

3.4. Design Parameter Dependency on Hydrophobicity.

In Figure 8, the theoretical contact angle dependencies on the design parameters of the trapezoid of the height (H), side angle (θ_{side}), and pitch (P), are analyzed and compared with the experimental data. The theoretical contact angles (θ_{app}) for the Wenzel state ($\theta_{\text{app}}^{\text{W}}$) and the Cassie–Baxter state ($\theta_{\text{app}}^{\text{CB}}$) are determined by the method described in section 3.2 after changing one of the design parameters.

As discussed in section 3.2, on a PDMS trapezoids surface where $H = 11.9 \mu\text{m}$, $\theta_{\text{side}} = 56^\circ$, $P = 40 \mu\text{m}$, and $W_t = 26 \mu\text{m}$, the sagging height (h) before and after the application of the Teflon coating is estimated to be 2.1 and $1.9 \mu\text{m}$, respectively. As liquid sagging occurs at the rounded region near the top surface ($h < 3.6 \mu\text{m}$), as shown in Case 1 in Figure 4c, $\theta_{\text{app}}^{\text{CB}}$ (dashed line) does not change as H or θ_{side} changes, as shown in Figure 8a–d. Regarding the superhydrophobicity of both PDMS trapezoids (before and after receiving a Teflon coating), there are stronger dependencies on H and P rather than on θ_{side} . In particular, as

shown in Figure 8c, a water droplet prefers the Wenzel state regardless of the value of θ_{side} on a fresh PDMS trapezoids surface when $H = 11.9 \mu\text{m}$, $P = 40 \mu\text{m}$, and $W_t = 26 \mu\text{m}$.

The role of θ_{side} is more critical in the realization of a superhydrophobic surface made of hydrophilic material¹² and in the implementation of a superoleophobic surface.^{13,14,17} According to Marmur's previous analysis,¹⁵ the liquid–air interface in the equilibrium state should be placed on the lower part of the convex microstructures, i.e., the sidewall of the PDMS trapezoids, for an oleophobic surface with a metastable Cassie–Baxter state. In general, a liquid droplet can stay in the Cassie–Baxter regime on the microstructured surface shown in Figure 4 only if $\theta_{\text{side}} \leq \theta_{\text{FLAT}} \leq 180^\circ$.³⁷ Particularly, in the case of methanol, which has a low surface tension ($\gamma_{\text{la}} = 22.7 \text{ mN/m}$), the contact angle (θ_{FLAT}) is 68° on a flat Teflon surface.¹⁷ Therefore, an overhanging angle (θ_{side}) of 56° in the PDMS trapezoids is a necessary condition to provide the Cassie–Baxter state for the oleophobic property. This condition was also verified by a Teflon-coated PDMS trapezoids surface with a θ_{side} value of 72° and a H value of $20 \mu\text{m}$, as shown in Figure 9. In our previous work,¹⁷ the PDMS trapezoids with a θ_{side} value of 56° and a H value of $11.9 \mu\text{m}$ has demonstrated

(37) Oliver, J. F.; Huh, C.; Mason, S. G. *J. Colloid Interface Sci.* **1977**, *59*(3), 568–581.

a contact angle of 135° with methanol as shown in Figure 10a. However, as θ_{side} is larger than the θ_{FLAT} value of methanol, the Teflon-coated PDMS trapezoids surface with a θ_{side} value of 72° does not show oleophobicity and has a close value of contact angle (70°) to that of a flat Teflon surface (68°) as shown in Figure 10b, despite the fact that those PDMS trapezoids are taller than PDMS trapezoids with a θ_{side} value of 56° . This can support the importance of the side angle of the overhang structure to accomplish oleophobicity. The fabrication method and characteristics of PDMS trapezoids with an increased height are discussed in section 3.5.

The graphs in Figure 8 clearly demonstrate that the most effective means of improving the hydrophobic property in microstructured surfaces is to enhance the intrinsic contact angle (θ_{FLAT}) of the structural surface. In Figure 8, it is noteworthy that the shift of the Wenzel curve (solid line) is larger than that of the Cassie–Baxter curve (dashed line) due to the intrinsic contact angle change (i.e., from the graphs in the left column to the graphs in the right column of Figure 8). However, the highest contact angle that is achievable by chemical modification was limited.⁴ Recently, a surface with double roughness⁹ was demonstrated to promote an intrinsic contact angle of the structural surface. In that study, a contact angle of 156° was achieved on a silanized rough surface fabricated by the XeF_2 etching of a Si substrate. Thus, this strongly suggests that refinement of the process of creating the PDMS trapezoids surface can improve its hydrophobicity considerably.

It is also important to emphasize that the fabricated PDMS trapezoids sample is, for the first time in this research field, almost exactly placed at the intersection of the curves of $\theta_{\text{app}}^{\text{W}}$ (solid line) and $\theta_{\text{app}}^{\text{CB}}$ (dashed line). The characteristic of the minimized contact angle difference ($\Delta\theta_{\text{app}}^{\text{W}} = \theta_{\text{app}}^{\text{CB}} \approx 1^\circ$, also see Figure 5d) implies that the superhydrophobic surface is robust²⁴ to external disturbances. Hence, the geometrical parameters in the fabricated Teflon-coated PDMS trapezoids are mostly optimized for the highest contact angle and for robust superhydrophobicity.

3.5. Analysis of the Increased Height Effect in PDMS Trapezoids. In order to validate the proposed analytical model, another surface was fabricated, as shown Figure 9, with an increased aspect ratio of the PDMS trapezoids patterns ($H = 20\ \mu\text{m}$, and $\theta_{\text{side}} = 72^\circ$). Microsized trapezoids were created using a negative photoresist AZ2070 (Clariant, Co. Ltd.) that was coated to a target thickness (11.9 or $20\ \mu\text{m}$) on a metal-patterned (180-nm -thick Cr) glass substrate, i.e., an embedded photomask. With backside exposure through the embedded photomask, an opal diffuser plate (NT02–149; Edmund Optics, Co. Ltd.) was inserted into the UV pathway to the embedded photomask so that the diffused light could form a photoresist with an inverse-trapezoidal cross-section. In this backside three-dimensional diffuser lithography,¹⁸ the sidewall profile could be adjusted by the refractive index of an index matching liquid that was located between the diffuser and the embedded Cr mask. Deionized water was used as the index matching liquid for $\theta_{\text{side}} = 56^\circ$, while no index matching liquid (i.e., air) was used for $\theta_{\text{side}} = 72^\circ$. During the backside three-dimensional diffuser lithography process, a large UV exposure dose ($10\,000\ \text{mJ}/\text{cm}^2$ with an index matching liquid of water, and $5000\ \text{mJ}/\text{cm}^2$ without an index matching liquid) was applied to create a straight sidewall line. After two consecutive PDMS replication processes,¹⁷ PDMS trapezoids surface was attained.

After a subsequent Teflon coating, the fabricated surface also showed a high contact angle, as shown in Figure 11. As in the previous sections, θ_{app} can be determined with the different geometrical figures of a trapezoid ($H = 20\ \mu\text{m}$ and $\theta_{\text{side}} = 72^\circ$), as shown in Figure 12. In this case, a fresh PDMS trapezoids surface has a θ_{app} value of 138.6° while a Teflon-coated trapezoids surface

has a θ_{app} value of 152.6° . The wetting behavior of the Teflon-coated trapezoids surface was modeled to be in the Cassie–Baxter state, as confirmed by a water droplet image. The inset of Figure 11 clearly shows the microstructures underneath the Cassie–Baxter droplet, which are visible because they are higher than those in Figure 4. However, the contact angle difference between two wetting states of the sample with an increased height ($H = 20\ \mu\text{m}$) was slightly larger than that of the control sample ($H = 11.9\ \mu\text{m}$) discussed in the previous section.

4. Conclusions

In this work, the first robust superhydrophobic property was reported on a flexible and transparent PDMS template with a perfectly ordered inverse-trapezoidal array. With the aid of analytical modeling and thermodynamical analysis of the fabricated PDMS trapezoids surface, the robustness of the superhydrophobicity and the dependencies of various design parameters (height, side angle, and pitch) on the superhydrophobic characteristics were comprehensively studied.

There are two important points regarding the robustness of superhydrophobic property. First, the Gibbs free energy analysis showed that the Cassie–Baxter state is thermodynamically favorable on the Teflon-coated PDMS trapezoids surface. This indicates that the superhydrophobicity is stable because the Wenzel droplet always transitions to the Cassie–Baxter state automatically. Therefore, the apparent contact angle does not change, even after external disturbances. Second, the wetting behavior of the fabricated PDMS trapezoids surface was placed very closely to the intersection of the Wenzel and the Cassie–Baxter curves with the aid of a fluoropolymer (Teflon) layer as well as by the precise engineering of the geometries in the PDMS trapezoids array. This ensures that the contact angle is not apparently changed, even when any type of wetting behavior transition occurs. The robustness of the superhydrophobicity on the Teflon-coated PDMS trapezoids surface was verified in an impinging test using a water droplet dropped at a high speed.

In terms of the design parameter dependencies, while the side angle did not show significant dependency on the superhydrophobic properties due to the presence of overhangs, the PDMS trapezoids surface was advantageous in supporting a droplet with a low surface tension when the side angle was low. Rather than the height or the side angle of the trapezoids structure, the intrinsic contact angle of the structural surface was the most critical parameter for the implementation of superhydrophobic surfaces.

Finally, the validity of thermodynamic analysis was also supported by another type of PDMS trapezoids surface with an increased height and a steeper side angle. As the Teflon-coated PDMS trapezoids surface has transparent and oleophobic properties together with robustness against external disturbances, its application can be useful in new areas such as a self-cleaning surface, a diving suit, a submarine application, and others.

Acknowledgment. This work was partially supported by a National Research Foundation of Korea (NRF) grant funded by the Korean Ministry of Education, Science and Technology (MEST) (No. 2009-0083079). It was also partially supported by the National Research and Development Program (NRDP, 2009-0065615) for the development of biomedical function monitoring biosensors, which was also funded by the Korean Ministry of Education, Science and Technology. M. Im would like to acknowledge the financial support from the Brain Korea 21 Project, the School of Information Technology, KAIST, in 2009. The authors would also like to thank Ju-Hyun Kim, Chunghee Park, and Professor Hoon Huh for their generous support regarding the high-speed camera imaging.